1000-0569/2007/023(01)-0073-82 *Acta Petrologica Sinica* 岩石学报

Silicate-salt(sulfate) liquid immiscibility: a study of melt inclusions in minerals of the Mushugai-Khuduk carbonatite-bearing complex (southern Mongolia)

Irina A. Andreeva[1*], Vyacheslav I. Kovalenko [1] and Vladimir B. Naumov [2]

1. *Institute of Geology of Ore Deposit, Petrography, Mineralogy, and Geochemistry, Russian Academy of Sciences, Staromonetnyi per.* 35, *Moscow* 109017, *Russia*
2. *Vernadsky Institute of Geochemistry and Analytical Chemistry, Russian Academy of Sciences, Kosygina* 19, *Moscow* 117334, *Russia*

Received: 2006-07-07, *Accepted*: 2006-11-10

Andreeva I A, Kovalenko V I and Naumov V B. 2007. Silicate-salt (sulfate) liquid immiscibility: a study of melt inclusions in minerals of the Mushugai-Khuduk carbonatite-bearing complex (southern Mongolia) *Acta Petrologica Sinica*, 23(1):73-82

Abstract Crystalline and melt inclusions were studied in garnet, diopside, potassium feldspar, and sphene from the garnet syenite porphyry of the carbonatite-bearing complex Mushugai-Khuduk, southern Mongolia. Phlogopite, clinopyroxene, albite, potassium feldspar, sphene, wollastonite, magnetite, Ca and Sr sulfates, fluorite, and apatite were identified among the crystalline inclusions. The melt inclusions were homogenized at 1010~1080℃ and analyzed on an electron microprobe. Silicate, salt, and combined silicate-salt melt inclusions were found. Silicate melts show considerable variations in SiO_2 concentration (56 to 66wt%), high $Na_2O + K_2O$ (up to 17wt%), and elevated Zr, F, and Cl contents. In terms of bulk rock chemistry, the silicate melts are alkali syenites. During thermometric experiments, salt melt inclusions quenched into homogeneous glasses of predominantly sulfate compositions containing no more than 1.3wt% SiO_2. These melts are enriched in alkalis, Ba, Sr, P, F, and Cl. The investigation of the silicate and salt melt inclusions in minerals of the garnet syenite porphyries indicate that these rocks were formed under influence of the processes of crystallization differentiation and magma separation into immiscible silicate and salt (sulfate) liquids.

Key words Alkaline rocks, Carbonatites, Silicate and salt melt inclusions, Crystal fractionation, Liquid immiscibility

1 Introduction

The complexes of alkaline igneous rocks and carbonatites have always attracted much attention of geologists and petrologists. Such complexes are important repositories of many trace components (REE, Nb, Ta, P, U, Th, Ba, Sr, Pb, Zn, etc.) and are often associated with economic deposits. In this context, an urgent task is the investigation of the compositions of ore-forming magmas and processes of ore component concentration in magmatic systems. This problem has been addressed by many researchers, and carbonatite-bearing alkaline complexes have been explored in the Kola Peninsula, East Pamirs, Aldan, southern Africa, etc. (Kogarko, 1999; Solovova *et al.*, 1996; Panina *et al.*, 1999; Solovova *et al.*, 1998). We studied previously the Late Mesozoic potassium alkaline carbonatite-bearing complex Mushugai-Khuduk in southern Mongolia and demonstrated that the alkaline and ore-bearing rocks (melanephelinite, leucite phonolite, shonkinite, theralite, quartz syenite, magnetite-apatite and celestite-fluorite rocks) of the complex were formed from silicate, silicate-salt (silicate-phosphate), and diverse salt melts (carbonate-phosphate, phosphate-sulfate, fluoride-sulfate, chloride-sulfate, etc.). It was also argued that the concentration of ore components in silicate melts up to economic levels was controlled by salt components (Andreeva *et al.*, 1995, 1996, 1998, 1999, 2003).

This paper presents the results of a study of melt inclusions in minerals of ore-bearing garnet syenite porphyries, which were found in the course of test drilling in the region of the Mushugai deposit. These peculiar rocks are composed of garnet crystals, up to 5~6cm in size, embedded in a fine-grained syenite groundmass. Up to now, their origin remained controversial (magmatic or metasomatic). Our investigation of melt inclusions allowed us to resolve this dilemma. We determined the physicochemical parameters and compositions of mineral-forming media for these rocks and outlined the processes responsible for their formation.

* E-mail: andreeva@igem.ru

2 Geologic background

The geologic setting of the Mushugai-Khuduk complex was described in detail by Samoilov and Kovalenko (1983). The rocks of the complex (volcanic and subvolcanic) cut a Paleozoic stratified volcanosedimentary sequence and are overlain by Early Cretaceous basalts. According to K-Ar and Rb-Sr isotopic data the age of the complex was estimated as the Late Jurassic to Early Cretaceous.

The complex is built up of diverse alkaline extrusive (including pyroclastic), subvolcanic, and intrusive alkaline and subalkaline rocks ranging in composition from melanephelinite and nepheline melaleucitite to trachyte and latite in the extrusive facies, and from shonkinite to quartz syenite in the plutonic facies. The alkaline magmatism is spatially and genetically linked with the formation of ore mineralization in the complex, including mineralized breccias with a carbonate cement, carbonatite, and apatite-rich rocks. Test and assessment drilling operations were performed in some areas of the Mushugai ore occurrence that showed the highest abundance of mineralized rocks. Some boreholes were drilled to depths of 70 ~ 300m. This activity revealed rare earth ores of various geochemical types. Some of them were previously described on the surface, and others were first found in drill cores. In general, there are two main types of ores: (1) carbonatitic and (2) apatite-bearing ores.

The composition of carbonatite-series rocks varies considerably owing to variations in the proportions of carbonate, fluorite, and quartz. There are continuous series from carbonatite proper to fluorite-dominated and siliceous rocks. The area of the Mushugai ore occurrence comprises approximately equal amounts of carbonatites proper and other members of the carbonatite association, such as magnetite-apatite, fluorite, celestite-fluorite, and other rocks.

The apatite-bearing REE ores include magnetite-apatite, apatite and phlogopite-apatite rocks, feldspar-apatite rocks, and alkaline rocks (syenite, syenite porphyry, etc.) containing abundant apatite and garnet megacrysts and schlieren of apatite-dominated rocks.

3 Description of the sample studied

Garnet syenite porphyry was recovered by drilling in a large (30 ~ 70m) stockwork apatite body in the eastern flank of the complex (Fig. 1) (Samoilov and Kovalenko, 1983). It is a light gray porphyritic rock with large garnet crystals (up to 5 ~ 6cm) in a fine-grained syenite groundmass. The phenocrysts of the syenite are dominated by potassium feldspar (40 ~ 45%), diopside (15 ~ 20%), and plagioclase (5 ~ 10%). The minor and accessory phases are sphene, phlogopite, amphibole, zircon, apatite, magnetite, ilmenite, and pyrite. Calcite, celestite, and fluorite were also detected as accessory phases. The chemical compositions of rock and rock-forming minerals are shown in Table 1.

Large garnet phenocrysts have a dark brown color. Their compositions correspond to the andradite-grossular series with high TiO_2 (up to 4wt%). Garnet crystals are often mantled by reaction rims of small garnet, diopside, sphene, and potassium

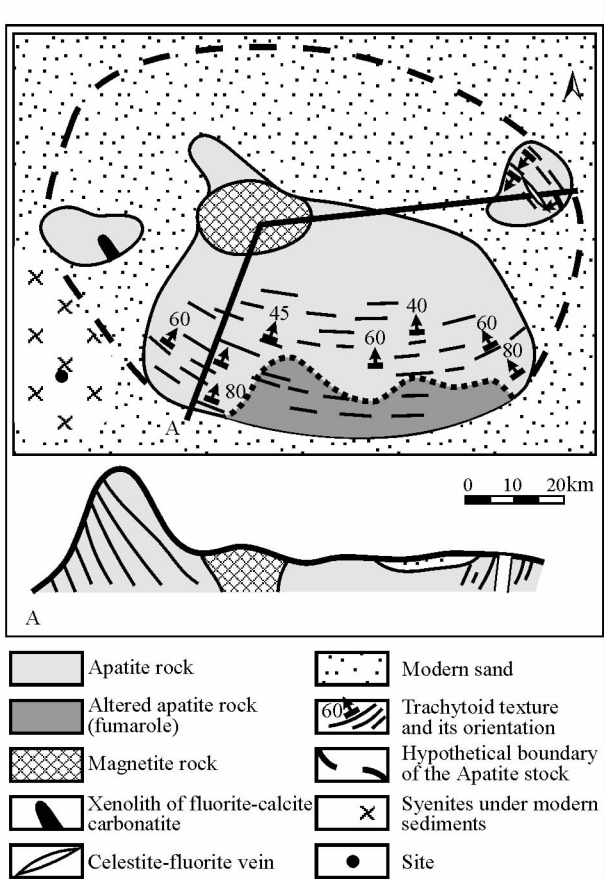

Fig. 1 Geological structure of the Apatite stock (Samoilov V. S., Kovalenko V. I., 1983).

feldspar grains. The garnet from the reaction rim is andradite with up to 5wt% TiO_2.

Diopside and plagioclase are euhedral with respect to the potassium feldspar. Diopside forms elongated prismatic crystals from 0.3 to 1.0 mm long. In places, the diopside is replaced by amphibole. Prismatic plagioclase crystals are 1 ~ 2mm in size, and their compositions correspond to oligoclase or albite.

Potassium feldspar crystals often show perthite structures and contain inclusions of clinopyroxene, sphene, fluorite, and magnetite. Their chemical compositions are characterized by high BaO (up to 0.8wt%) and SrO (up to 1.1wt%) contents.

Sphene and apatite are the most abundant minor minerals. Sphene forms light yellow wedge-shaped crystals, up to 0.8 mm in size, which are often associated with diopside and plagioclase. The sphene shows high concentrations of ZrO_2 (up to 2.9wt%), $Ce_2O_3 + La_2O_3$ (up to 2wt%), Nb_2O_5 (0.7 ~ 1.2wt%), Nd_2O_3 (up to 0.7wt%), and BaO (up to 0.7wt%) (Table 1). Sphene of similar composition was found by us in a theralite from this complex (Andreeva *et al.*, 1999).

Apatite forms either small euhedral crystals, sometimes intergrown with diopside, or aggregates of larger grains in potassium feldspar. In addition, apatite occurs in association with fine-grained calcite, which often forms aggregates up to 2mm in size. The mineral is F-apatite (2.9 ~ 4.0wt% F) with high concentrations of SrO (up to 0.64wt%), $Ce_2O_3 + La_2O_3$ (up to 1wt%), and S (up to 0.3wt%). In addition to fluorapatite, the rock contains a phosphate mineral whose composition

Table 1 Chemical compositions (wt%) of rock and minerals of the garnet syenite porphyry

	1	2	3	4	5	6	7	8	9	10	11
SiO_2	43.35	49.72	39.51	63.19	65.90	65.30	30.01	36.00	34.44	7.33	0.12
TiO_2	1.10	0.39	4.82	0.02	0.07	0.04	32.06	3.95	4.81	0.01	0.00
Al_2O_3	11.35	1.68	14.69	25.20	19.97	20.46	1.12	10.57	3.63	0.10	0.04
FeO	7.61	15.80	10.19	0.68	1.24	0.14	2.16	14.71	21.92	0.02	0.00
MnO	0.18	0.45	0.14	0.02	0.01	0.00	0.07	0.27	0.16	0.00	0.02
MgO	0.45	7.39	17.95	0.14	1.00	0.00	0.00	0.62	0.39	0.02	0.00
BaO	0.31	0.00	1.14	—	—	0.00	0.67	0.04	—	0.00	0.53
SrO	1.22	0.00	—	—	—	0.00	—	0.00	—	0.10	54.98
CaO	18.56	23.10	0.00	5.73	0.33	0.14	26.50	34.32	32.15	47.75	0.14
Na_2O	3.61	0.86	0.42	6.31	10.58	0.91	0.07	0.00	0.06	0.32	0.05
K_2O	2.22	0.02	8.71	0.27	0.96	13.88	0.05	0.00	0.08	0.10	0.04
P_2O_5	1.34	0.00	0.00	0.00	0.00	0.00	0.00	0.00	—	27.02	—
Ce_2O_3	—	0.00	0.39	—	—	0.00	1.25	0.01	—	5.21	0.00
La_2O_3	—	0.00	0.04	—	—	0.00	0.24	0.00	—	2.61	0.00
ZrO_2	—	—	0.00	—	—	0.00	2.13	—	—	—	—
Nb_2O_5	—	—	0.02	—	—	—	1.18	—	—	—	—
Nd_2O_3	—	—	0.00	—	—	—	0.69	—	—	—	—
F	0.27	0.02	0.37	—	—	—	0.24	—	—	2.88	—
Cl	0.00	0.01	0.01	0.02	0.00	0.01	0.05	0.00	0.00	0.00	0.00
S	0.43	0.00	0.02	0.01	0.00	0.00	0.01	0.01	0.01	0.90	44.18 *
Total	100.40	99.44	98.42	101.59	100.06	100.88	98.50	100.50	97.65	94.37	100.10

Note: FeO is total iron. (1) Whole rock; the total sum includes 1.91wt% H_2O, 3.87wt% CO_2, and 1.62wt% of REE; (2) diopside; (3) phlogopite; (4) oligoclase; (5) albite; (6) potassium feldspar; (7) sphene; (8), (9) garnet; (10) F-apatite; (11) celestite.
* Concentration is given in the form of SO_3.

is intermediate between apatite and britholite. The latter is rich in Ce_2O_3 + La_2O_3 (up to 8wt%) and S (up to 0.9wt%) and contains 27wt% P_2O_5 and 7wt% SiO_2.

Phlogopite is not very common in the rock and forms flakes up to 0.5 mm in size. It is rich in TiO_2 (up to 5wt%) and BaO (up to 1.1wt%). Zircon, celestite, and fluorite form small crystals usually occurring as inclusions in potassium feldspar.

The opaque minerals of the rock are represented by magnetite, ilmenite, and pyrite. They occur as irregular grains in potassium feldspar, often in association with celestite and apatite.

The groundmass of the garnet-bearing syenite porphyry is dominated by potassium feldspar and plagioclase with minor amounts of small grains of opaque mineral. The potassium feldspar crystals of the groundmass are up to 0.1 ~ 0.2mm in size and often show perthite structures. Albitic plagioclase forms tabular crystals.

In general, the mineralogy and chemistry of the rock are similar to those of the rare garnet syenite variety that was described in 1921 under the name sviatonossite by Eskola (1921).

4 Experimental methods

Inclusions in minerals were examined optically in double-polished sections, 0.3mm thick. Thermometric experiments were performed in resistance furnaces and a Linkam TS 1500 microscopic heating stage designed for high temperatures. Temperature was measured with an error of 10℃. In order to reach equilibrium between melt and the host mineral, the samples were kept for 30 min in resistance furnaces under the desired temperature.

The compositions of glasses of homogenized melt inclusions, daughter phases in the inclusions, crystalline inclusions, and rock-forming minerals were determined by X-ray spectral electron probe microanalysis (EPMA). The measurements were conducted at an accelerating voltage of 15kV and a beam current of 30 nA. The glasses of melt inclusions were analyzed by rastering over an area of 12 × 12, 5 × 5 or 2 × 2μm. The daughter minerals of melt inclusions and crystalline inclusions were analyzed either with a focused beam or by rastering over an area of 5 × 5 or 2 × 2μm. Rock-forming minerals were also analyzed in raster areas of 5 × 5μm.

5 Results of inclusion study.

Primary magmatic inclusions were explored in diopside, sphene, potassium feldspar, and garnet. Crystalline and melt inclusions were distinguished on the basis of phase composition. It is worth mentioning that data on melt inclusions in garnet are very scarce in the literature (Chupin *et al.*, 2001; Titov *et al.*, 2001; Panina *et al.*, 2001).

5.1 Crystalline Inclusions

Crystalline inclusions were studied in diopside, sphene, potassium feldspar, and garnet. Both silicate and nonsilicate phases were detected: phlogopite, clinopyroxene, albite, potassium feldspar, sphene, wollastonite, magnetite, Ca sulfate, celestite, calcite, fluorite, apatite, and an apatite-group phosphate. The composition of this phosphate is intermediate between apatite and britholite. The chemical compositions of crystalline inclusions are shown in Table 2.

Table 2 Chemical compositions (wt %) of crystalline inclusions in the minerals of garnet syenite porphyry

	1	2	3	4	5	6	7	8	9	10	11	12	13	14
SiO_2	48.00	47.94	38.00	64.16	62.03	67.20	29.59	30.35	1.98	10.78	0.75	51.58	0.55	0.34
TiO_2	0.38	1.16	4.70	0.03	0.05	0.03	35.46	32.04	0.25	0.04	0.01	0.11	0.05	0.72
Al_2O_3	3.94	3.05	13.45	19.14	18.45	19.64	1.20	1.50	0.14	0.15	0.04	0.15	0.20	0.06
FeO	16.82	14.61	12.45	0.28	0.64	0.91	1.82	2.57	0.77	0.58	0.79	0.62	0.55	0.25
MnO	0.48	0.38	0.27	0.00	0.00	0.06	0.04	0.00	0.00	0.09	0.01	0.16	0.08	0.06
MgO	7.21	7.99	14.72	0.01	0.27	0.10	0.05	0.02	0.24	0.00	0.19	0.21	0.00	0.04
CaO	22.11	21.61	0.39	0.43	0.64	0.64	26.10	24.92	51.20	46.64	61.51	47.52	39.57	0.86
BaO	0.09	0.05	0.24	—	0.30	0.00	0.62	0.34	—	0.07	—	0.00	0.00	1.24
SrO	0.04	0.00	0.29	—	0.24	0.00	0.03	0.21	—	0.44	—	0.07	1.52	69.60
Na_2O	1.50	1.07	0.90	1.46	3.11	10.48	0.00	0.02	0.61	0.12	0.07	0.00	0.02	0.08
K_2O	0.01	0.14	11.13	15.19	14.12	1.45	0.00	0.32	0.13	0.00	0.01	0.02	0.12	0.01
P_2O_5	0.00	0.00	0.00	0.01	0.00	0.01	0.02	0.01	40.99	20.70	0.00	0.02	0.01	0.00
Ce_2O_3	0.00	0.00	0.10	—	0.17	0.00	1.34	1.93	0.87	6.93	—	0.00	0.02	0.58
La_2O_3	0.00	0.00	0.01	—	0.00	0.00	0.34	0.55	0.43	2.74	—	0.00	0.00	0.06
ZrO_2	0.00	0.15	0.01	—	0.08	0.00	3.67	3.43	—	—	—	—	—	0.00
F	0.05	0.00	4.91	—	0.48	0.00	0.20	0.53	3.01	2.73	0.00	0.01	0.07	0.00
Cl	0.00	0.00	0.01	0.02	0.00	0.03	0.00	0.00	0.04	0.25	0.02	0.00	0.18	0.01
S	0.00	0.00	0.03	0.00	0.10	0.00	0.01	0.02	0.33	2.78	0.01	0.00	47.45*	26.40*
Total	100.63	98.15	101.62	100.75	100.68	100.54	100.49	98.75	100.98	100.31	63.44	100.47	90.39	100.31
Host mineral	Grt	Kfs	Di	Grt	Di	Di	Di	Kfs	Di	Grt	Di	Grt	Grt	Sph

Note: FeO is total iron. (1), (2) diopside; (3) phlogopite; (4), (5) potassium feldspar; (6) albite; (7), (8) sphene; (9) F-apatite; (10) phosphate phase (the total sum includes 0.23wt% UO_2, 2.41wt% ThO_2, 1.71wt% Nd_2O_3, 0.92wt% Sm_2O_3; (11) calcite; (12) wollastonite; (13) Ca sulfate; (14) celestite. Host minerals: Grt, garnet; Kfs, potassium feldspar; Di, diopside; Sph, sphen.
* Concentration is given in the form of SO_3.

5.2 Melt Inclusions

Primary melt inclusions were found in all the major rock-forming minerals: diopside, potassium feldspar, garnet, and sphene. They are represented by silicate (in diopside, sphene, and potassium feldspar) and salt (in diopside and garnet) melts. Combined silicate-salt inclusions were found in the garnet. Silicate and salt melt inclusions are completely crystallized and randomly distributed. Their sizes vary from 20 to 50μm. Combined silicate-salt inclusions have sizes of 50 ~ 80μm. The compositions of daughter minerals in the melt inclusions and homogenized glasses of these inclusions are shown in Table 3, 4.

Table 3 Chemical compositions (wt %) of glasses from homogenized melt inclusions in the diopside, sphene, and potassium feldspar from garnet syenite porphyry

	1	2	3	4	5	6	7	8	9
SiO_2	56.66	61.33	60.90	0.95	62.34	66.37	64.19	63.78	63.91
TiO_2	0.78	1.08	0.59	0.00	0.92	1.43	1.61	0.17	0.06
Al_2O_3	15.49	15.60	15.58	—	17.97	18.10	17.04	18.17	17.90
FeO	3.71	5.04	3.68	0.94	0.23	1.39	1.38	3.20	2.83
MnO	0.08	0.11	0.10	—	0.00	0.06	0.05	0.06	0.00
MgO	2.23	3.07	1.89	—	0.07	0.27	0.09	0.41	0.67
CaO	6.74	3.19	4.92	30.61	1.20	2.01	2.45	2.81	3.12
BaO	0.04	0.08	0.04	0.60	0.03	0.00	0.05	0.30	0.34
SrO	0.31	0.00	0.08	1.76	0.15	0.00	0.10	0.37	0.17
Na_2O	2.58	2.98	3.30	5.03	4.31	4.17	3.56	4.19	4.76
K_2O	9.74	5.97	8.29	7.14	9.79	6.24	7.06	7.33	7.31
P_2O_5	0.00	0.08	0.01	1.23	0.02	0.01	0.02	0.01	0.04
Ce_2O_3	0.07	0.10	0.08	0.40	0.58	0.10	0.17	0.14	0.16
La_2O_3	0.01	0.01	0.02	0.13	0.57	0.07	0.14	0.00	0.06
ZrO_2	0.11	0.20	0.11	—	0.32	0.85	0.42	0.08	0.13
F	1.12	1.58	0.89	1.96	0.75	0.95	0.58	0.02	0.28
Cl	0.18	0.15	0.15	—	0.03	0.04	0.09	0.02	0.00
S	0.07	0.14	0.11	42.62	0.05	0.03	0.09	0.03	0.02
Total	99.92	100.71	99.94	93.37	96.88	100.13	99.09	101.09	101.76
Host mineral	Di	Di	Di (6)*	Di	Sph	Sph	Sph (7)*	Kfs	Kfs

Note: FeO is total iron. (1) ~ (3) daughter minerals of melt inclusions: (1), (2) Na-Ca sulfate; (3) calcite. (4) ~ (9) homogenized glasses of salt melt inclusions in garnet.

Table 4 Chemical composition (wt %) of daughter minerals of salt melt inclusions and glasses from homogenized salt melt inclusions in garnet from garnet syenite porphyry

	1	2	3	4	5	6	7	8	9
CaO	35.62	45.02	58.51	32.95	32.47	31.35	34.40	34.10	39.42
Na_2O	8.50	3.04	0.02	4.70	2.88	5.55	3.02	2.50	3.02
K_2O	0.20	0.63	0.00	4.25	3.73	3.43	3.11	4.63	3.09
BaO	0.04	0.00	0.05	0.60	0.99	0.09	1.26	0.59	1.48
SrO	0.50	0.87	0.09	1.72	2.23	1.50	1.59	1.95	3.73
SO_3	38.90	37.27	0.05	40.42	45.67	42.30	38.77	39.47	31.22
F	1.81	3.45	0.00	1.88	3.21	1.68	3.81	1.16	4.62
Cl	0.27	0.41	0.02	1.01	1.22	1.02	0.63	1.19	0.84
SiO_2	0.51	0.30	0.47	0.64	0.52	0.39	0.52	0.52	1.29
TiO_2	0.01	0.06	0.03	0.05	0.05	0.02	0.00	0.03	0.21
Al_2O_3	0.17	0.12	0.24	0.15	0.19	0.14	0.44	0.09	0.35
FeO	0.46	0.37	0.42	0.44	0.45	0.44	0.67	0.36	0.75
MnO	0.09	0.05	0.00	0.05	0.06	0.03	0.11	0.05	0.01
MgO	0.00	0.03	0.00	0.21	0.17	0.00	0.28	0.23	0.15
P_2O_5	0.00	0.00	0.00	0.56	0.36	0.37	0.34	0.47	0.35
Ce_2O_3	0.00	0.02	0.00	0.20	0.35	0.21	0.48	0.22	0.46
La_2O_3	0.00	0.03	0.04	0.00	0.02	0.02	0.08	0.10	0.07
Total	87.08	91.65	59.94	89.83	94.57	88.54	89.51	87.66	91.07

Note: FeO is total iron. (1) ~ (3) daughter minerals of melt inclusions: (1), (2) Na-Ca sulfate; (3) calcite. (4) ~ (9) homogenized glasses of salt melt inclusions in garnet.

As was mentioned above, silicate and salt melt inclusions were detected in diopside. Inclusions of both types were observed in some growth zones of the diopside, which suggests their cogenetic character. All the inclusions have irregular shapes with uneven boundaries, and their gas phase is not clearly discernible. The inclusions are filled with a mineral aggregate composed of isotropic and anisotropic phases. Among the crystalline phases of silicate inclusions, an amphibole-like mineral, mica, and calcite were analyzed. The daughter minerals of the salt inclusions were not identified because of the small sizes of individual grains.

Melting of phases in the silicate inclusions began at a temperature of 840℃, when the gas phase acquired a spherical shape. The last solid daughter phase melted in the inclusions at a temperature of 950 ~ 970℃. The silicate inclusions were completely homogenized at 1010 ~ 1080℃. The homogenization temperatures of the salt melt inclusions in diopside were 1060 ~ 1080℃.

Melt inclusions in sphene and potassium feldspar have negative crystal shapes and sizes of 10 ~ 40μm. Similar to the diopside-hosted inclusions, these inclusions are composed of fine-grained aggregates of isotropic and anisotropic daughter crystals, which prevented their microprobe analysis. The inclusions in sphene were completely homogenized at temperatures of 1010 ~ 1030℃, and those in potassium feldspar, at 1040℃.

Garnets contain numerous primary melt inclusions, among which salt and combined silicate-salt melt inclusions were recognized. Salt melt inclusions are randomly distributed within phenocrysts and some grains contain dozens of such inclusions. The inclusions are 20 ~ 50μm in size, they are usually irregular, occasionally rounded or partially faced. Combined silicate-salt inclusions are much rarer. They are usually rounded or, occasionally, tubular. Their size varies from 50 to 35 × 80μm.

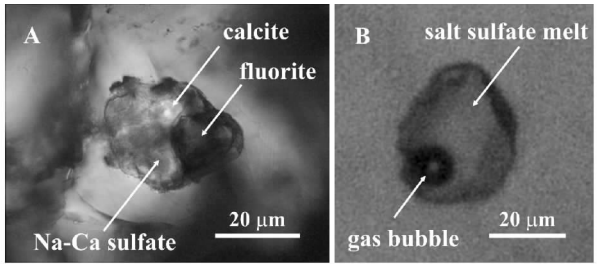

Fig. 2 Inclusions of salt sulfate melt in garnet from the garnet syenite porphyry: (A) initial, before heating; (B) after thermometric experiment at 950℃ and 1 atm.

The salt inclusions are completely crystallized, and their gas phase is deformed and poorly discernible (Fig. 2). Fluorite and calcite were reliably identified among the daughter minerals. In addition, we analyzed a Na-Ca sulfate phase, which occupies a significant fraction of inclusion volume. A similar phase was previously found among the daughter minerals of fluoride-sulfate and chloride-sulfate inclusions in fluorite from the celestite-fluorite ore of the Mushugai-Khuduk complex (Andreeva *et al.*, 1998). It should be noted that the totals of analyses of the Na-Ca sulfate phase were much lower than 100%, which is indicative of the presence of water in its composition. This is indirectly supported by its unstable behavior under the electron beam. The following changes were observed in the phase composition of inclusions during experiments in the microscopic heating stage. The earliest evidence for melting of crystalline phases was observed at 570℃, and the gas bubble acquired a regular spherical shape at 650℃. The solid phases were completely resorbed at 930 ~ 940℃, after which the inclusions contained only liquid and gas phases. The salt melt inclusions homogenized at temperatures of 1050 ~ 1070℃. During the subsequent

cooling, a gas bubble reappeared at 930 ~ 910℃, and a fine-grained aggregate was eventually formed.

Thermometric experiments with the same inclusions were conducted in an electric furnace, which allowed rapid quenching (1 ~ 2s). These experiments led to unexpected results. The salt inclusions in garnet and diopside were quenched into a homogeneous glass after heating up to 930 ~ 950℃.

Combined silicate-salt inclusions are characterized by the presence of a garnet rim (up to 5vol%) on the walls of vacuoles. The composition of garnet in the rim corresponds to grossular. In addition to garnet, the silicate mineral assemblage of the inclusions contains potassium feldspar and albite. The salt phases include a sulfate mineral close to gypsum in composition, calcite, and several phosphate minerals. The latter include apatite, a mineral intermediate between apatite and britholite, and a monazite-like phosphate (Table 5). Apatite proper is represented by fluorine variety and contains up to 11wt% REE (Ce_2O_3 + La_2O_3) and up to 0.45wt% S. The phosphate phase intermediate between apatite and britholite is also enriched in REE (Ce_2O_3 + La_2O_3), S (up to 1.5wt%), and SiO_2 (8.4wt%). The monazite-like mineral contains 30wt% Ce_2O_3 + La_2O_3, 13.4wt% ThO_2, 5.6wt% Nd_2O_3, 1.33wt% Sm_2O_3, and 0.45wt% UO_2 (Table 5, an. 7). These inclusions were never homogenized during thermometric experiments.

Thus, the thermometric investigation of melt inclusions in the minerals of the garnet syenite porphyry suggested that the phenocrysts of this rock crystallized at temperatures of 1080 ~ 1010℃.

Table 5 Chemical composition (wt %) of daughter minerals of the combined silicate – salt melt inclusions in garnet from garnet syenite porphyry

	1	2	3	4	5	6	7	8	9
SiO_2	65.89	65.72	37.66	2.12	2.32	8.42	0.86	0.96	0.30
TiO_2	0.01	0.02	0.29	0.00	0.04	0.00	0.04	0.01	0.06
Al_2O_3	19.55	21.27	21.61	0.02	0.17	0.19	0.10	0.11	0.12
FeO	0.29	0.27	1.78	0.14	0.80		0.69	1.36	0.37
MnO	0.00	0.02	0.19	0.00	0.03	0.02	0.00	1.30	0.05
MgO	0.01	0.02	0.03	0.02	0.00	0.00	0.00	0.65	0.03
CaO	0.50	0.86	39.68	51.55	46.21	47.50	10.85	62.70	45.02
BaO	0.07	0.00	0.01	0.01	0.01	0.08	0.06	0.00	0.00
SrO	0.00	0.00	0.00	0.00	0.26	0.23	2.21	0.10	0.87
Na_2O	0.62	10.18	0.05	0.16	0.02	0.19	0.02	0.05	3.04
K_2O	13.19	0.19	0.00	0.01	0.02	0.03	0.00	0.11	0.63
P_2O_5	0.00	0.02	0.00	37.92	37.08	26.57	29.49	0.04	0.41
Ce_2O_3	—	—	—	2.57	7.56	6.11	20.75	—	0.02
La_2O_3	—	—	—	0.97	3.56	2.74	9.28	—	0.03
F	—	—	—	2.79	3.24	2.90	3.40	—	3.45
Cl	0.00	0.01	0.01	0.04	0.00	0.03	0.00	0.00	0.41
S	0.00	0.01	0.00	0.35	0.45	1.53	1.28	0.13	37,27*
Total	100.13	98.59	101.31	98.67	101.77	97.17	97.81	67.52	97.16

Note: FeO is total iron. (1) potassium feldspar; (2) albite; (3) garnet; (4), (5) F-apatite; (6), (7) phosphate phases, (7) the total sum includes 0.45wt% UO_2, 13.39wt% ThO_2, 5.61wt% Nd_2O_3, 1.33wt% Sm_2O_3; (8) calcite; (9) sulfate phase.

* Concentration is given in the form of SO_3.

6 Compositions of Melt Inclusions

6.1 Silicate melts

The SiO_2 content of homogenized melt inclusions varies from 56 to 66wt%, and the most significant variations were observed in the inclusions in clinopyroxene (from 56 to 63wt%). All the melts trapped in diopside, sphene, and potassium feldspar are very rich in alkalis. The sum of alkalis ranges from 9 to 17wt%, and K_2O is strongly predominant in the inclusions in diopside (K_2O/Na_2O ~ 3) (Table 3).

The compositions of homogenized glasses of melt inclusions in each mineral show some specific features. For instance, homogenized glasses from inclusions in diopside are enriched relative to the average syenite composition in FeO (up to 6wt%), CaO (3 ~ 7wt%), ZrO_2 (up to 0.2wt%), F (up to 1.6wt%), and Cl (up to 0.2wt%).

Similar to inclusions in diopside, the melts in sphene are variable in SiO_2 and Al_2O_3 contents (62 ~ 66wt% and 15 ~ 19.5wt%, respectively). In addition, they show relatively high concentrations of FeO (up to 2.7wt%), TiO_2 (up to 2.8wt%), and CaO (3 ~ 7wt%) and very low MgO concentrations (0.03 ~ 0.08wt%). By comparison with the clinopyroxene-hosted inclusions, the melts trapped in sphene are significantly richer in ZrO_2 (up to 0.8wt%), which suggests a higher degree of differentiation. The concentrations of volatile components (F and Cl) in the glasses trapped in sphene are also high (0.95 and 0.16wt%, respectively), although they are lower than those in the clinopyroxene-hosted melt inclusions.

The homogenized glasses in the potassic feldspar show elevated contents of FeO (3wt%), CaO (3wt%), BaO (0.3wt%), ZrO_2 (up to 0.13wt%) and low contents of TiO_2 (0.06 ~ 0.2wt%) and MgO (0.4 ~ 0.7wt%) with average

concentrations of SiO_2 of 64wt% and Al_2O_3 of 18wt%. The concentrations of Cl in the melts are no higher than a few hundredths of percent and F varies from hundredths to 0.3wt%.

Overall, all the silicate melts in diopside, sphene, and potassium feldspar of the garnet syenite porphyry fall into the alkali syenite field on the TAS classification diagram.

6.2 Salt melts

Salt melt inclusions found in two minerals, diopside and garnet. Salt melt inclusions coexist with silicate melt inclusions in some diopside grains. The compositions of salt melts trapped in diopside (Table 3, an. 7) and garnet (Table 4) are identical. The major components are CaO (32 ~ 38wt%) and SO_3 (37 ~ 40wt%). Similar to the silicate melts, the sulfate melts are enriched in alkalis (up to 8wt% in total), SrO (up to 3.7wt%), BaO (up to 1.5wt%), P_2O_5 (up to 1.2wt%), F (up to 3.8wt%), and Cl (up to 1.2wt%). The low totals of components in the microprobe analyses of homogenized inclusions in both garnet and diopside imply significant concentrations of H_2O and CO_2. This suggestion is supported by the occurrence among the daughter minerals of considerable amounts of a hydrous sulfate phase and calcite.

7 Discussion

The investigation of melt inclusions in the minerals of the garnet syenite porphyry demonstrated that this rock crystallized from silicate and salt melts. Silicate melt inclusions were found in the diopside, sphene, and potassium feldspar phenocrysts. The microprobe examination of homogenized glasses from these inclusions revealed considerable variations in SiO_2, from 56 to 66wt%. The glasses show high concentrations of alkalis (Na_2O + K_2O up to 17wt%), ZrO_2, F, and Cl. Most of the silicate melts fall within the field of alkali syenites.

Salt melt inclusions were found in diopside and garnet. All the salt melts have a sulfate-dominated composition with no more than 1.3wt% SiO_2. The salt melts are also rich in alkalis, BaO, SrO, P_2O_5, F, and Cl. The salt inclusions in diopside associate with silicate melt inclusions, which suggests the coexistence of immiscible silicate and salt melts during the crystallization of this mineral. It should be noted however that pure silicate melt inclusions were never found in garnet.

Nonetheless, there are several lines of evidence that, similar to diopside, the garnet of this rock crystallized in equilibrium with silicate and salt melts. Among them are the occurrence of combined silicate-salt inclusions in garnet, the presence of cogenetic silicate and salt inclusions in single diopside grains, the similar homogenization temperatures of silicate and salt melt inclusions in diopside and salt inclusions in garnet, and the identical compositions of salt melt inclusions in the two minerals. The mechanism of selective entrapment of one of two coexisting liquids by minerals is not yet understood. However, such relationships were previously noted by Roedder (1984).

Cases of silicate-sulphate immiscibility were recorded by K. Torok (2003) during study of clinopyroxene megacrysts from basalt tuff of Szentbekkalla in western Hungary.

Table 6 Calculated composition (wt%) of salt melts in minerals from the ore-bearing rocks of the Mushugai-Khuduk complex

	1	2	3	4
CaO	35.00	26.00	44.00	54.50
BaO	1.20	1.90	0.49	—
SrO	9.90	5.70	6.00	—
Na_2O	2.70	11.10	—	0.10
K_2O	3.90	3.70	—	—
SO_3	33.10	29.00	24.90	0.50
P_2O_5	—	—	17.00	17.60
F	5.50	2.10	3.71	1.80
Cl	0.10	10.90	0.05	—
CO_2	2.10	4.50	1.92	19.70
H_2O	6.00	4.70	—	—
SiO_2	—	—	0.46	0.80
TiO_2	—	—	—	—
Al_2O_3	—	—	—	—
FeO	—	—	0.48	2.60
MgO	—	—	—	—
Ce_2O_3	0.20	0.10	0.68	1.7
La_2O_3	0.30	0.30	0.31	0.70
Total	100.00	100.00	100.00	100.00

Note: (1) Fluoride-sulphate; (2) chloride-sulphate; (3) phosphate-sulphate; (4) phosphate-carbonate melts.

A remarkable feature of the salt inclusions in garnet and diopside is their ability to quench into a glass in thermometric experiments, which provides a unique opportunity to accurately analyze the salt melts. As we noted above, salt melts of similar compositions (fluoride-sulfate and chloride-sulfate) were studied by us in fluorite from the celestite-fluorite ores of the Mushugai-Khuduk complex (Table 6) (Andreeva *et al.*, 1998). Thermometric experiments with these inclusions were performed in a microscopic heating stage, which did not allow rapid quenching after homogenization. The cooling lasted 1 ~ 2min, which was sufficient for the complete crystallization of inclusions. Because of this, the composition of salt melt trapped in fluorite was roughly estimated from phase proportions and compositions. Since the salt melt inclusions in garnet were quenched into a clear glass in experiments in an electric furnace allowing rapid quenching (1 ~ 2s), we used the same procedure with the sulfate inclusions in fluorite from the celestite-fluorite ore. The new experiments were carried out at temperatures of 600 ~ 670℃ based on our previous observations. After quenching, the inclusions showed varying phase composition. The largest inclusions (30 ~ 40μm) were composed of aggregates of quench crystals, whereas smaller inclusions (up to 20μm) often yielded glass with microliths of quench phases and, occasionally, homogeneous glass (Fig. 3). These observations allowed us to conclude that the salt melts of such compositions could be quenched to homogeneous glasses under certain conditions.

The experimental study by Jones and Wyllie (1983) of the multicomponent system $CaCO_3$-$Ca(OH)_2$-CaF_2-$BaSO_4$-$La(OH)_3$ containing 31.2wt% $CaCO_3$, 24.9wt% $Ca(OH)_2$, 13.5wt% CaF, 10.4wt% $BaSO_4$, and 20wt% $La(OH)_3$ confirmed the possibility of formation of salt glasses. These authors obtained carbonate-dominated glasses of the following composition at temperatures of 650 ~ 543℃ and a pressure of

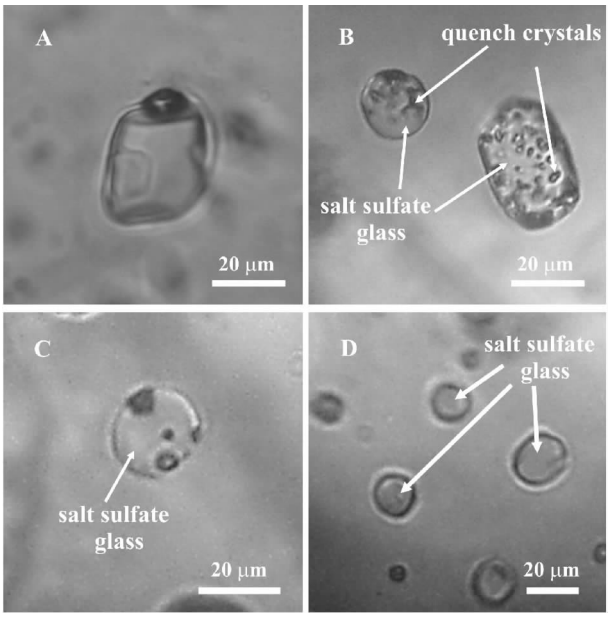

Fig. 3 Inclusions of salt sulfate melt in fluorite from celestite-fluorite rock: (A)) initial, before heating; (B), (C), (D) after thermometric experiment at 680℃ and 1 atm.

1kbar: 45.0wt% CaO, 6.59wt% BaO, 18.2wt% La_2O_3, 3.08wt% SO_3, and 6.2wt% F (total without CO_2, H_2O, and O = F is 76.46wt%). Since glass formation was never reported in similar systems without $BaSO_4$ and $La(OH)_3$, in which synthetic liquids were always quenched to crystalline aggregates, the authors conjectured that the main factor of glass formation is the presence in the system of La, Ba, and, probably, SO_4 in certain proportions. The glasses from sulfate inclusions in clinopyroxene and garnet of the syenite porphyry also showed high concentrations of BaO and SrO comprising together up to 5.5wt%, and elevated concentrations of Ce and La (up to 0.5wt%), although they are not so high as in the experimental carbonate glasses. Thus, it cannot be excluded that the formation of salt glass during quenching of homogenized melt inclusions was primarily related to the influence of the aforementioned components and SO_4.

Variation diagrams of major and minor elements against SiO_2 for the glasses of homogenized melt inclusions display distinct trends in the behavior of some major and volatile components (Al_2O_3, FeO, CaO, ZrO_2, F, and Cl) during syenite melt evolution. The results are illustrated in Fig. 4. The concentration of alumina increases with increasing SiO_2, which is controlled by garnet and clinopyroxene crystallization. A positive correlation between SiO_2 and ZrO_2 also suggests gradual accumulation of zirconium in the residual silicate melt in the course of differentiation. The highest ZrO_2 contents of 0.5 ~ 0.8wt% were detected in the most evolved compositions.

The abundances of FeO, CaO, F, and Cl show different trends. These components are negatively correlated with SiO_2 concentration. The depletion in FeO during melt evolution is a consequence of garnet and clinopyroxene fractionation. These minerals were also responsible for the CaO-SiO_2 fractionation trend, with minor roles of apatite, calcite, and salt melt. A considerable decrease in the concentrations of volatile

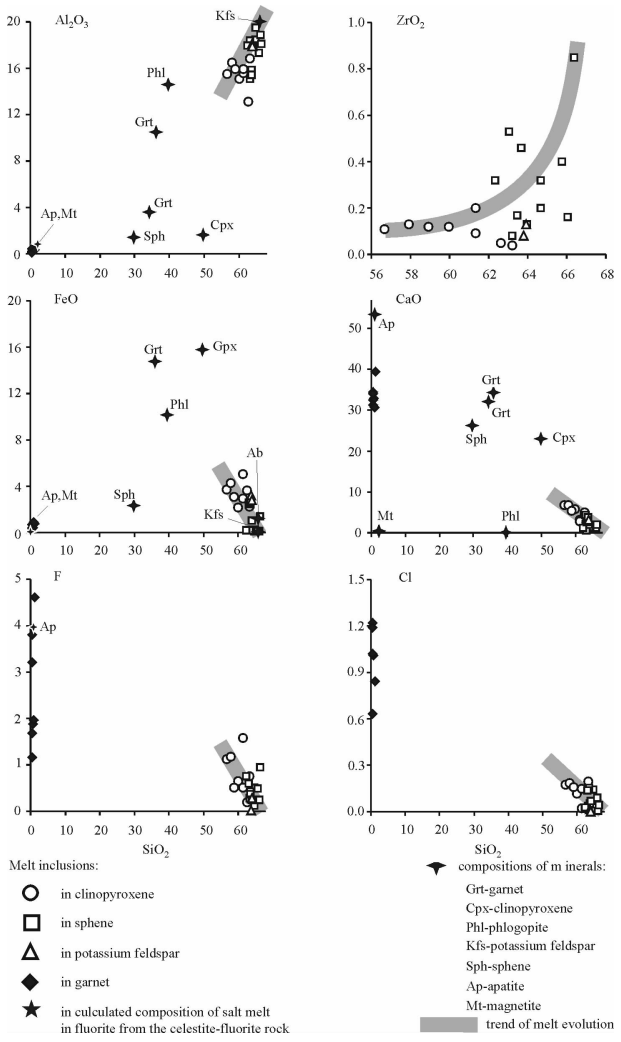

Fig. 4 Variations of melt inclusion compositions (wt%) in the minerals of garnet syenite porphyry versus SiO_2 concentration in the melt.

components (F and Cl) in melts with increasing SiO_2 content could be related to the separation of salt melt, which extracted these components already at early stages of syenite magma crystallization. In addition, the depletion of melts in F and Cl was probably due to fractionation of some other minerals, in particular, fluorite and apatite.

A characteristic feature of all the melts studied, both silicate and salt, is their fluorine-rich compositions. The analysis of the behavior of various components as functions of fluorine concentration is therefore of particular interest. The diagrams of Fig. 5 show that the silicate melts tend to become depleted in alumina and alkalis and enriched in CaO and Cl with increasing fluorine concentration.

The salt melts show a distinct decrease in K_2O content with increasing F. As to Na_2O, the compositions of salt melts form two trends. One of them shows a dramatic increase in Na_2O with increasing F concentration, which could result in the appearance of williaumite. Kogarko (1977) argued that an immiscible fluoride liquid saturated in NaF could be separated from alkaline melts during the late stages of crystallization of agpaitic nepheline

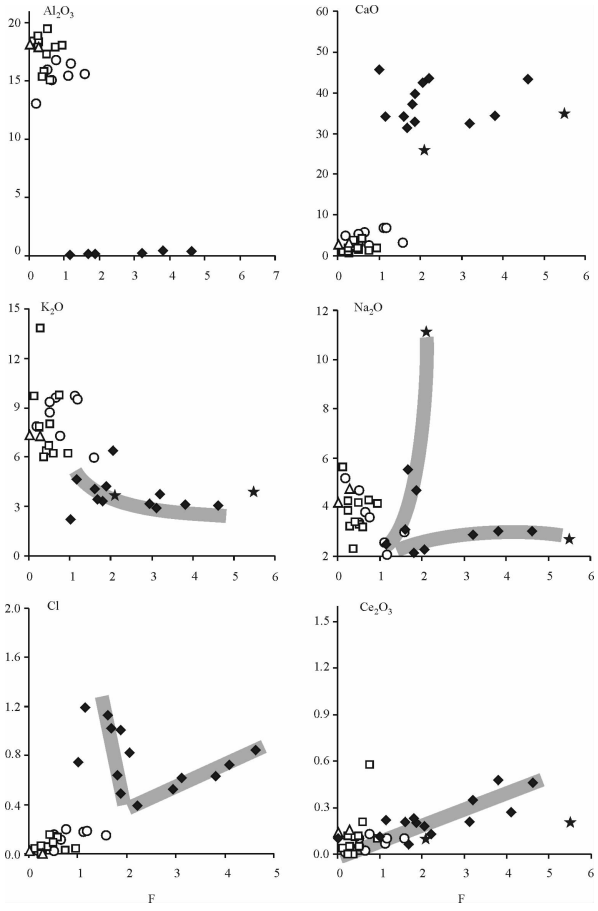

Fig. 5 Variations of melt inclusion compositions (wt%) in the minerals of garnet syenite porphyry versus F concentration in the melt. Symbol as in Fig. 3.

syenites. The second trend is formed by salt melts showing an increase in Na_2O content at a relatively constant F concentration.

The behavior of Cl as a function of F concentration is similar to that of Na. There are also two groups of melts, one of which exhibits Cl accumulation with increasing F content, and the other shows a negative F-Cl correlation. The existence of two tendencies for the salt melts is probably related to the separation of the sulfate melt enriched in F and Cl into two liquids of fluoride-sulfate and chloride-sulfate compositions, which were found by us in the celestite-fluorite ores of the complex studied. This is illustrated by the F-Na_2O diagram (Fig. 5), where the compositions of fluoride-sulfate and chloride-sulfate melts lie on the extensions of the two trends.

Of particular interest is the behavior of REE in the silicate and salt melts. Figure 4 exhibits a strong positive correlation between Ce_2O_3 and F, which suggests that the degree of melt enrichment in cerium is a function of fluorine content. The maximum concentrations of Ce_2O_3 (0.5wt%) and F (4.6wt%) were measured in the salt melts. This could lead to the crystallization of REE carbonates, fluorapatite, fluorite, and, probably, cerium fluoride (fluorcerite) from these liquids. This allows us to connect the genesis of REE-bearing carbonatites and various fluoride ores, which defined the metallogenic signature of the Mushugai-Khuduk complex, with the salt melts considered in this study.

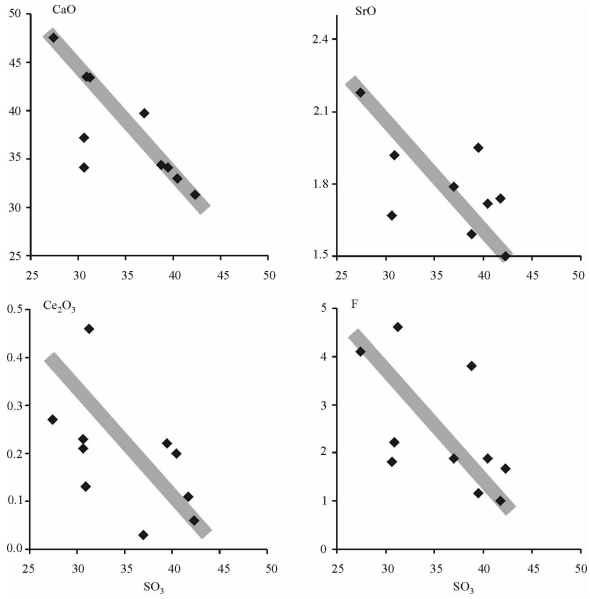

Fig. 6 Variations of melt inclusion compositions (wt%) in the minerals of garnet syenite porphyry versus SO_3 concentration in the melt. Symbol as in Fig. 3.

Taking into account the sulfate-dominated chemistry of the salt melts, we examined correlations between various components and SO_3 concentrations. Figure 6 shows that the concentrations of CaO, SrO, Ce_2O_3, and F in the inclusions decrease in general with decreasing SO_3 content. Of particular importance is the behavior of Ce_2O_3 and F versus sulfur, which again highlights the key role of fluorine in the accumulation of REE in salt melts.

Thus, the analysis of the chemical characteristics of silicate and salt melts suggests that the rock studied was formed under the influence of two major magmatic processes, crystal fractionation and liquid immiscibility. The high concentrations of volatile components, in particular fluorine and chlorine, in the alkali syenite magma played probably the main role in the separation of salt melts, which extracted considerable amounts of calcium, alkalis, sulfur, phosphorus, rare (Ba and Sr) and rare earth elements (Ce), fluorine, and chlorine.

8 Conclusions

We studied crystalline and melt inclusions in garnet, diopside, potassium feldspar, and sphene from the garnet syenite porphyry of the Mushugai-Khuduk carbonatite-bearing complex in southern Mongolia. Phlogopite, clinopyroxene, albite, potassium feldspar, sphene, wollastonite, magnetite, Ca and Sr sulfates, calcite, fluorite, and apatite were determined among the crystalline inclusions. The melt inclusions represented by silicate and salt melts and show homogenization temperatures of 1010 ~ 1080℃. Silicate melt inclusions were found in diopside, potassium feldspar, and sphene. They have variable SiO_2 content, from 56 to 66wt%, and show high $Na_2O + K_2O$ (up to 17wt%), Zr, F, and Cl concentrations. In general the silicate melts are chemically similar to alkali syenite. Salt melt inclusions were found in diopside and garnet. In the course of thermometric experiments, they produced homogeneous quench

glasses of sulfate-dominated compositions with SiO_2 content no higher than 1.3wt%. These melts are strongly enriched in Ba, Sr, P, F, and Cl. Our study of salt melt inclusions demonstrated that fluorine played a leading role in the accumulation of light lanthanides, in particular Ce_2O_3, in sulfate salt melts.

The investigation of the silicate and salt melt inclusions led us to the conclusions that the garnet syenite porphyry was formed under the influence of the processes of crystallization differentiation and magma unmixing into immiscible silicate and salt (sulfate) liquids.

Acknowledgement This study was financially supported by the Russian Foundation for Basic Research, project nos. 05-05-64055, 05-05-62056, 07-05-00497.

References

Andreeva IA, Naumov VB, Kovalenko VI, Listratova EN, Kononkova NN. 1995. Magmatic celestite in melt inclusions in apatite from the Mushugai-Khuduk alkali volcanoplutonic complex in southern Mongolia. Trans. (Doklady) USSR Acad. Sci., 339 A: 154 – 159

Andreeva IA, Naumov VB, Kovalenko VI, Kononkova NN. 1996. Natural phosphate-silicate melts. Trans. (Doklady) USSR Acad. Sci., 345: 247 – 252

Andreeva IA, Naumov VB, Kovalenko VI, Kononkova NN. 1998. Fluoride-sulfate and chloride-sulfate salt melts of the Mushugai-Khuduk carbonatite-bearing complex, southern Mongolia. Petrologiya, (6): 307 – 315

Andreeva IA, Naumov VB, Kovalenko VI, Kononkova NN. 1999. Magma composition and the genesis of theralites from the Mushugai-Khuduk carbonatite - bearing complex, southern Mongolia. Geokhimiya, (8): 826 – 841

Andreeva IA, Kovalenko VI. 2003. Magma compositions and genesis of the rocks of the Mushugai-Khuduk carbonatite-bearing alkaline complex (southern Mongolia): evidence from melt inclusions. Per. Mineral., 72: 95 – 105

Chupin VP, Kuzmin DV, Touret J. 2001. High-pressure melt and fluid inclusions in minerals of garnet granulites/eclogites (eastern Pamir). XVI European Current Research o Fluid Inclusions Abstracts, Porto., pp. 95 – 98

Escola P. 1921. On the igneous rocks of Sviatoy Noss in Transbaikalia Overs. Fiuska Vetensk. Soc. Forhandl, 63, Afa A.,1, pp. 1 – 101

Jones AP, Wyllie PJ. 1983. Low-temperature glass quenched from a synthetic, rare earth carbonatite: implications for the origin of the Mountain Pass deposit, California. Econom. Geol., 78: 1721 – 1723

Kogarko LN. 1977. Problemy genezisa agpaitovykh magm (Problems of the genesis of agpaitic magmas). Nauka, Moscow, 294 p

Kogarko LN. 1999. Problems of the genesis of giant apatite and rare-metal deposits in the Kola Peninsula, Russia. Geol. Rudn. Mestorozhd., 41: 387 – 403.

Panina LI, Usoltseva LM. 1999. Alkaline high-Ca carbonate melt inclusions in melilite-monticellite-olivine rocks from the Malomurunskii alkaline massif, Aldan. Petrology, (7): 610 – 625

Panina LI, Sazonov AM, Usol'zeva LM. 2001. Melilitic and monticheliteb-earing rocks of the Krestovskaya intrusion (northern Siberian Platform) and their genesis. Geol. Geofiz., 42: 1314 – 1332

Roedder E. 1984. Fluid inclusions. Reviews in Mineralogy, Vol. 12, Book Crafters, Michigan

Samoilov VS, Kovalenko VI. 1983. Kompleksy shchelochnykh porod i karbonatitov Mongolii (Alkali and carbonatite complexes of Mongolia). Nauka, Moscow, 196p

Solovova IP, Girnis AV, Ryabchikov ID. 1996. Inclusions of carbonate and silicate melts in minerals of alkali basaltoids from the eastern Pamirs. Petrology, (4): 319 – 341

Solovova IP, Ryabchikov ID, Kogarko LN, Kononkova NN. 1998. Inclusions in minerals of the Palaborwa carbonatite complex, south Africa. Geochemistry International, 36: 377 – 388

Titov AV, Khromykh SV, Vladimirov AG, Pospelova LN. 2001. Melt inclusions in garnet and quartz from dacite porphyries of the Actobe Structure, Kazakhstan: estimation of generation conditions and composition of primary melts. Trans. (Doklady) Russ. Acad. Sci.: Earth. Sci. Sec., 377: 229 – 233

Torok K, Bali E, Szabo C, Szakal JA. 2003. Sr-barite droplets associated with sulfide blebs in clinopiroxene megacrysts from basaltic tuff (Szentbekkalla, western Hungary). Lithos, 66: 275 – 289